Acta Cryst. (1998). B**54**, 391–398

The Yttrium Oxide Fluoride Solid Solution Described as a Composite Modulated System

SIEGBERT SCHMID

Research School of Chemistry, Australian National University, GPO Box 414, Canberra, ACT 2601, Australia. E-mail: schmid@rsc.anu.edu.au

(*Received 6 October 1997; accepted 16 February 1998*)

Abstract

Single-crystal X-ray diffraction data (Mo $K\alpha$ radiation) are used to determine the structure of the $\Delta = 0.174$ member of a $(YO_{1-\Delta}F_{\Delta})F_{1+\Delta}$, $0.12 \leq \Delta \leq 0.22$, wide-range non-stoichiometric solid solution in the yttrium oxide fluoride system. The structure is refined as a composite modulated structure composed of two mutually incommensurable Q and H substructures with overall superspace-group symmetry *Acmm*-(0,0,1.174..)0*s*0. The Q substructure has lattice parameters $a = 5.415$ (2), $b_Q = 5.534$ (2) and $c_Q = 5.525$ (2) Å, and superspace-group symmetry *Acmm*(0,0,1.174..)0*s*0. The H substructure has lattice parameters $a = 5.415$ (2), $b_H = 1/2b_Q = 2.767$ (1) and $c_H = 4.696$ (2) Å, and superspace-group symmetry *Pmcm*(0,1/2,0.8518...)*s*00. Refinement on 338 unique reflections converged to $R = 0.025$, while a previous conventional superstructure refinement led to $R = 0.101$. This lowering of the R factor goes hand-in-hand with a substantial reduction in the number of refined parameters.

1. Introduction

A large number of recent publications reflect the importance currently attributed to composite modulated structures. Several review articles have dealt with general crystallographic aspects (van Smaalen, 1995; Yamamoto, 1996), and structures and physical properties (Wiegers, 1996). It has been shown that a description as a composite modulated structure has advantages over classic crystallography in many cases. The description as a composite modulated structure is especially useful for compounds within wide-range solid solutions. Atomic modulation functions (AMF's) describe the deviation from the average of any atom-based parameter at a given point in the structure. It has been shown for a number of systems, *e.g.* zirconium nitride oxide fluoride (Schmid & Withers, 1996), tantalum tungsten oxide (Schmid *et al.*, 1996) and zirconium niobium oxide (Schmid *et al.*, 1997), that the AMF's are essentially the same for any structure within a particular solid solution field. Therefore, all structures within such a solid solution can be calculated, given that the magnitude of the primary modulation wavevector for a specific composition and the modulation functions for one example are known.

One of the systems that has been investigated in great detail is the zirconium nitride oxide fluoride system $(ZrN_{1-\Delta/2-z}F_{\Delta/2-z}O_{2z})F_{1+\Delta}$, with $0.12 \leq \Delta \leq 0.25$ (Jung & Juza, 1973; Withers *et al.*, 1993; Schlichenmaier *et al.*, 1993; Schmid & Withers, 1994, 1995, 1996). It was shown for the $\Delta = 0.185$ member that refinement as a composite modulated structure was superior to an atom-based superstructure refinement (Schmid & Withers, 1996). In particular, the overall R value for the refinement was lowered substantially, while at the same time reducing the number of positional parameters by almost an order of magnitude.

A similar anion-excess, fluorite-related solid solution occurs in the yttrium oxide fluoride system for an anion-to-cation ratio from 2.12 to 2.22 (*i.e.* $MX_{2+\Delta}$, $0.12 \leq \Delta \leq 0.22$). A detailed study of the yttrium oxide fluoride system by Mann & Bevan (1972) showed that each and every composition had its own unique structure, which were nonetheless closely related to each other. This solid solution has been described as being isostructural to the zirconium nitride oxide fluoride system (Makovicky & Hyde, 1981).

There have been conventional single-crystal X-ray structure refinements at four compositions within the range of this solid solution (Bevan & Mann, 1975; Bevan *et al.*, 1990). These compositions $Y_5O_4F_7$, $Y_6O_5F_8$, $Y_7O_6F_9$ and $Y_{17}O_{14}F_{23}$ correspond to an anion-to-cation ratio of 2.2, ~2.167, ~2.143 and ~2.176, *i.e.* $\Delta = 0.2$, 0.167, 0.143 and 0.176, respectively. The resultant structures were described as anion-excess, 'orthorhombic, one-dimensional superstructures of the fluorite-type subcell'. Although the superstructure approximations were apparently quite valid, the need for a refinement using the modulated structure approach has been discussed by Bevan *et al.* (1990).

The structures of $Y_7O_6F_9$ and $Zr_{108}N_{98}F_{138}$ were used to establish the concept of so-called vernier phases (Hyde *et al.*, 1974). In general terms, all such structures can be described as inorganic misfit layer compounds characterized by a strictly alternate stacking of two chemically different types of layers (Makovicky & Hyde, 1992). While the vernier concept was very useful to understand these structures, it limits the description to mutually commensurate layers. For zirconium nitride

oxide fluoride it has been shown that the solid solution is best described as an incommensurate composite modulated phase (Withers *et al.*, 1993) composed of two layers, *i.e.* substructures (*Q* and *H*; Guinier, 1984), which are mutually commensurable along their *a*- and *b*-axis directions, but whose relative periodicity along their collinear *c*-axis directions is linearly dependent on the anion-to-cation ratio (Schmid & Withers, 1994).

For yttrium oxide fluoride (as for zirconium nitride oxide fluoride) these substructures can be described as a layer of pseudo-tetragonal edge-sharing anion-centred metal tetrahedra (a 4^4 net of anions sandwiched between similar, but lower, density nets of cations, *i.e.* a {100} layer of fluorite-type; *Q* substructure) and a pseudo-hexagonal 3^6 net of anions (*H* substructure). The general stoichiometry with respect to these two subsystems is given as $(YO_{1-\Delta}F_{\Delta})F_{1+\Delta}$, with $0.12 \leq \Delta \leq 0.22$ (*Q* substructure in parentheses). The *H* substructure has to accommodate $1 + \Delta$ anions (where Δ is the number of additional anions with respect to the fluorite structure). The parameter Δ and, therefore, the stoichiometry, can be determined directly from the ratio of the average substructure *c*-axis dimensions c_Q/c_H. Plotting average substructure unit-cell dimensions (Bevan *et al.*, 1990) as a function of composition shows that the variable stoichiometry is almost solely accommodated by variation in the *H* substructure *c*-axis dimension (Fig. 1).

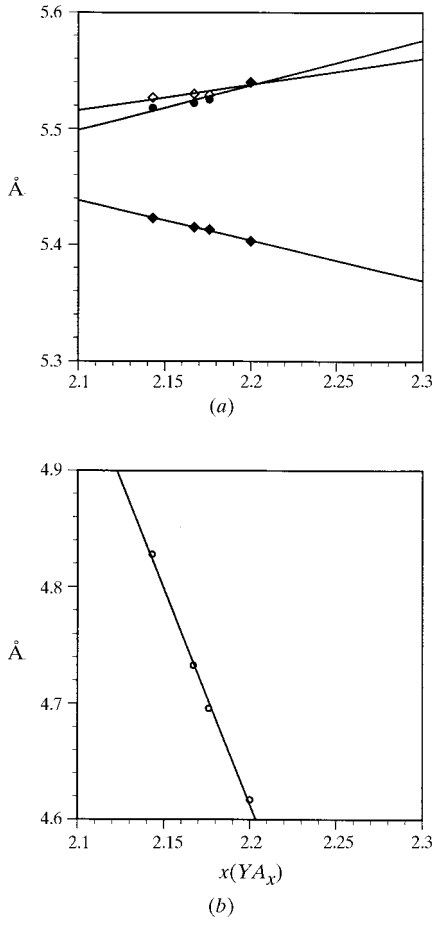

Fig. 1. Plot of (*a*) $\mathbf{a}_Q$ (filled diamond), $\mathbf{b}_Q$ (open diamond), $\mathbf{c}_Q$ (filled circle) and (*b*) $\mathbf{c}_H$ (open circle) substructure unit-cell dimensions as a function of composition (supercell dimensions from Bevan *et al.*, 1990). While there is only little change in the *Q* substructure cell dimensions, there is a dramatic decrease in the *H* substructure *c* dimension with increasing anion excess (~5%).

While the modulated structure approach is useful for all compositions within a solid solution, it is especially useful for compositions which otherwise need to be described as long-period superstructures. It is the large number of unobserved satellite reflections that cause correlations between structural parameters which make the least-squares refinement of such structures in terms of a conventional superstructure difficult. It was, therefore, considered to be most instructive to re-investigate the structure in the yttrium oxide fluoride system with the composition that displayed the longest superstructure, *i.e.* $Y_{17}O_{14}F_{23}$.

The purpose of this paper is to present the results of a single-crystal X-ray structure refinement of $(YO_{1-\Delta}F_{\Delta})F_{1+\Delta}$, $\Delta = 0.174$ (see §3) using the superspace-group approach, examine the crystal chemistry that follows from this refinement and compare these results with those of the 'isostructural' zirconium nitride oxide fluoride. The yttrium oxide fluoride system is expected to have a more straightforward crystal chemistry owing to the fact that there are only two types of anions.

2. Symmetry considerations

The overall superspace-group symmetry of this phase, both underlying parent substructures ($a_Q = a_H$, $b_Q = 2b_H$, $c_Q = \gamma c_H$) and the analytic form of the AMF's (Pérez-Mato *et al.*, 1987) describing the mutual influence of the two parent substructures upon each other have been determined previously (Withers *et al.*, 1993). The primary modulation wavevectors characteristic of the *Q* and *H* substructures were chosen as $\mathbf{q}_Q = \mathbf{c}_H^* - 2\mathbf{c}_Q^*$ and $\mathbf{q}_H = 1/2\mathbf{b}_H^* + \mathbf{c}_H^* - \mathbf{c}_Q^*$. Following the convention originally proposed by de Wolff *et al.* (1981) and, more recently, by Janssen *et al.* (1992), the true unit cell of the H parent substructure (Fig. 2; Fig. 1 in Withers *et al.*, 1993) has been doubled along the *b* direction so that the rational component of $\mathbf{q}_H$ becomes an integer with respect to the above basis set. The primary modulation wavevectors are now given by $\mathbf{q}_Q = \mathbf{c}_H{}^*$ and $\mathbf{q}_H = \mathbf{c}_Q{}^*$.

The characteristic extinction conditions when indexed with respect to the *Q* substructure, *i.e.* when all reflections are indexed as $(hklm)_Q = h\mathbf{a}_Q^* + k\mathbf{b}_Q^* + l\mathbf{c}_Q^* + m\mathbf{q}_Q$, are $F(hklm)_Q = 0$ unless $k + l = 2n$, $F(0klm)_Q = 0$ unless k, $l = 2n$ and $F(h0lm)_Q = 0$ unless l, $m = 2n$. These conditions imply a centring in superspace of the form $\{x_1, x_2 + \frac{1}{2}, x_3 + \frac{1}{2}, x_4\}_Q$, a hyper-glide plane $\{-x_1, x_2 + \frac{1}{2}, x_3,$

Table 1. *Important parameters*

Formula	$(YO_{1-\Delta}F_{\Delta})F_{1+\Delta}$, $\Delta = 0.174$
Superspace group	$Acmm(0,0,1.174..)0s0$ (No. 67.10)
Cell dimensions (Å)	$a = 5.415$ (2)
	$b = 5.534$ (2)
	$c_Q = 5.525$ (2), $c_H = 4.706$ (2)
Volume (Å^3)	165.57
Formula weight	127.73
Z	4
Density (g cm^{-3})	5.12
Wavelength (Å)	0.71069 (Mo $K\alpha$)
Monochromator	Graphite
Scan mode	$\omega/2\theta$ scans
Scan width (° in ω)	$0.8 + 0.35\tan\theta$
Scan speed (° min^{-1})	1.5
Attenuation factor	16.04
μ (cm^{-1})	348.20
θ range (°)	1.5–30
hklm range	$-7 \rightarrow h \rightarrow 7$
	$-7 \rightarrow k \rightarrow 7$
	$-11 \rightarrow l \rightarrow 10$
	$-2 \rightarrow m \rightarrow 4$
No. of measured/allowed reflections	12 123/5489
Reflections with $I > 3\sigma(I)$ all/unique	1829/338
Absorption correction	Gaussian ($14 \times 14 \times 14$ grid)
Transmission factors	$0.229 \leq A \leq 0.410$
Extinction correction	Isotropic, type II, 0.14 (1)

Table 2. *Refinement statistics for incommensurate model*

δ	0	
No. of refined parameters	28	
Weight	$1/\sigma(F)^2 + 0.001F^2$	
Residuals *R*, *wR*		
Overall	0.0245	0.0242
$m = 0$	0.0143	0.0176
$m = 1$	0.0413	0.0355
$m = 2$	0.119	0.144
$m = 3$	0.147	0.163

$x_4\}_Q$ and a hyper-glide plane of the form $\{x_1, -x_2 + \frac{1}{2}, x_3, x_4 + \frac{1}{2}\}_Q$, respectively. Overall *mmm* diffraction symmetry requires that superspace-group symmetry operations which map $\mathbf{q}_Q$ into $-\mathbf{q}_Q$, *e.g.* $\{-x_1, -x_2, -x_3, -x_4 + 2\delta\}_Q$ must also exist. The parameter δ fixes the relative positioning of the two component substructures (Fig. 2). These symmetry operations together generate the superspace group $Acmm(00\gamma)0s0$ (no. 67.10; Janssen *et al.*, 1992) for the Q substructure and, by definition, for the composite structure.

The two component substructures are related by the matrix W (see van Smaalen, 1991), transforming the Q substructure into the H substructure, given by

$$W = \begin{pmatrix} 1 & 0 & 0 & 0 \\ 0 & 1 & 0 & 0 \\ 0 & 0 & 0 & 1 \\ 0 & 0 & 1 & 0 \end{pmatrix}, \text{ with}$$

$$(\mathbf{a}^*, \mathbf{b}^*, \mathbf{c}^*, \mathbf{q})_H = (\mathbf{a}^*, \mathbf{b}^*, \mathbf{c}^*, \mathbf{q})_Q W^T,$$

where W^T is the transposed matrix. Owing to the doubling of the H substructure along the b direction, no standard superspace-group symbol can be given. The superspace group of the true H substructure with $a_Q = a_H$, $b_Q = 2b_H$, $c_Q = \gamma c_H$ is $Pmcm(0,\frac{1}{2},1/\gamma)s00$ (no. 51.16; Janssen *et al.*, 1992).

For mutually incommensurable substructures all possible relative origins of the two substructures occur at some point in the overall crystal so that the parameter δ can be freely chosen. For commensurable substructures, the choice of δ determines the resultant three-dimensional space-group symmetry (van Smaalen, 1995; Pérez-Mato, 1991).

The $M1$ (Y; site symmetry $2mm$) and $A1$ (0.826 O/0.174 F; site symmetry 222) sites of the average Q substructure occur with fractional coordinates given by $x, \frac{1}{4}, 0$ and $0, 0, -\frac{1}{4}$, respectively ($x \simeq -0.21$), while the $A1$ (F; site symmetry $m2m$) site of the average H substructure now occurs with fractional coordinates given by $\frac{1}{2}, y, \delta - \frac{1}{4}$ ($y \simeq -\frac{1}{8}$; see Fig. 2 and Table 2). Consequently, the allowed displacements associated with even- and odd-order modulation waves are constrained (Withers *et al.*, 1993). With respect to the above origin, the displacive AMF's describing the structural deviation of the $M1$ and $A1$ atoms away from

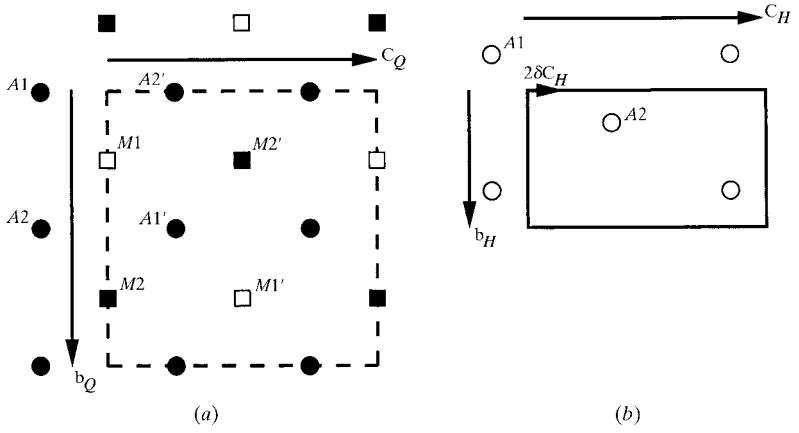

Fig. 2. Schematic representations of (*a*) the Q substructure and (*b*) the H substructure for yttrium oxide fluoride in projection along **a**. The inversion centres of the two substructures are displaced by $2\delta c_H$. Metal atoms are shown as squares ($M1$: open; $M2$: filled) and anions as circles (Q substructure: filled; H substructure: open).

their positions in the average Q substructure are given by

$$\begin{aligned}\mathbf{u}_{M1}(\mathbf{r}_{M1}+\mathbf{T}_Q) = &+\mathbf{a}_Q \sum_{2n=2,4..} \epsilon_{Mx}(2n\mathbf{q}_Q)\\ &\times \cos(2n.2\pi\{\mathbf{q}_Q.[\mathbf{r}_{M1}+\mathbf{T}_Q]-\delta\})\\ &-\mathbf{b}_Q \sum_{2n+1=1,3..} \epsilon_{My}([2n+1]\mathbf{q}_Q)\\ &\times \sin([2n+1].2\pi\{\mathbf{q}_Q.[\mathbf{r}_{M1}+\mathbf{T}_Q]-\delta\})\\ &-\mathbf{c}_Q \sum_{2n=2,4..} \epsilon_{Mz}(2n\mathbf{q}_Q)\\ &\times \sin(2n.2\pi\{\mathbf{q}_Q.[\mathbf{r}_{M1}+\mathbf{T}_Q]-\delta\}) \quad (1)\end{aligned}$$

$$\begin{aligned}\mathbf{u}_{A1}(\mathbf{r}_{A1}+\mathbf{T}_Q) = &-\mathbf{a}_Q \sum_{2n+1=1,3..} \epsilon_{Ax}([2n+1]\mathbf{q}_Q)\\ &\times \cos([2n+1].2\pi\{\mathbf{q}_Q.[\mathbf{r}_{A1}+\mathbf{T}_Q]-\delta\})\\ &+\mathbf{b}_Q \sum_{2n+1=1,3..} \epsilon_{Ay}([2n+1]\mathbf{q}_Q)\\ &\times \sin([2n+1].2\pi\{\mathbf{q}_Q.[\mathbf{r}_{A1}+\mathbf{T}_Q]-\delta\})\\ &-\mathbf{c}_Q \sum_{2n=2,4..} \epsilon_{Az}(2n\mathbf{q}_Q)\\ &\times \sin(2n.2\pi\{\mathbf{q}_Q.[\mathbf{r}_{A1}+\mathbf{T}_Q]-\delta\}), \quad (2)\end{aligned}$$

where $\mathbf{T}_Q$ is a Bravais lattice vector of the Q substructure and $n = m_Q$ is an integer which labels the harmonic order of the corresponding modulation wave with respect to the underlying Q substructure. The corresponding displacive AMF's describing the structural deviation of the $A1$ atoms away from their positions in the average H substructure are given by

$$\begin{aligned}\mathbf{u}_{A1}(\mathbf{r}_{A1}+\mathbf{T}_H) = &+\mathbf{a}_H \sum_{2n+1=1,3..} \epsilon_{Ax}([2n+1]\mathbf{q}_H)\\ &\times \cos(n\pi+[2n+1].2\pi\{\mathbf{q}_H.[\mathbf{r}_{A1}+\mathbf{T}_H]\})\\ &+\mathbf{b}_H \sum_{2n=2,4..} \epsilon_{Ay}(2n\mathbf{q}_H)\\ &\times \cos(n\pi+2n.2\pi\{\mathbf{q}_H.[\mathbf{r}_{A1}+\mathbf{T}_H]\})\\ &+\mathbf{c}_H \sum_{2n=2,4..} \epsilon_{Az}(2n\mathbf{q}_H)\\ &\times \sin(n\pi+2n.2\pi\{\mathbf{q}_H.[\mathbf{r}_{A1}+\mathbf{T}_H]\}), \quad (3)\end{aligned}$$

where $\mathbf{T}_H$ is a Bravais lattice vector of the H substructure (including the translation $\mathbf{b}_H = \frac{1}{2}\mathbf{b}_Q$) and $n = m_H$ is an integer which labels the harmonic order of the corresponding modulation wave with respect to the underlying H substructure.

3. Intensity measurement and data processing

Single crystals of nominal composition $(Y_{17}F_3O_{14})F_{20}$ were provided by Bevan *et al.* (1990). Accurate lattice parameters for Q and H substructures (see Table 1) were obtained from a least-squares fit of the setting angles for 25 reflections (each) with 2θ values between 15–26 and 17–45°, respectively, for Mo $K\alpha$ radiation. The single crystal used for data collection gave the c-axis ratio of the Q and H substructures as 1.174 to 1, slightly different to the nominal value of 1.1765 to 1, with the former used for subsequent data collection. For data collection a Philips PW1100/20 diffractometer was used. Background counting time was 10 s on either side of the scan. Square slits subtended angles $1 \times 1°$ at the crystal.

Table 3. *Coordinates of the average structure and displacive Fourier terms (in fractional coordinates)*

Y x, $\frac{1}{4}$, 0	−0.21144 (8)	
$\varepsilon_x(2\mathbf{q})$, $\varepsilon_x(4\mathbf{q})$	−0.0018 (3)	–
$\varepsilon_y(\mathbf{q})$, $\varepsilon_y(3\mathbf{q})$	0.0330 (1)	0.0067 (4)
$\varepsilon_z(2\mathbf{q})$, $\varepsilon_z(4\mathbf{q})$	0.0067 (2)	–
O 0, 0, $-\frac{1}{4}$		
$\varepsilon_x(\mathbf{q})$, $\varepsilon_x(3\mathbf{q})$	−0.0463 (9)	0.006 (3)
$\varepsilon_y(\mathbf{q})$, $\varepsilon_y(3\mathbf{q})$	−0.0201 (8)	0.006 (3)
$\varepsilon_z(2\mathbf{q})$, $\varepsilon_z(4\mathbf{q})$	−0.005 (1)	
F $\frac{1}{2}$ y, $-\frac{1}{4}$	−0.1158 (7)	
$\varepsilon_x(\mathbf{q})$, $\varepsilon_x(3\mathbf{q})$	0.1044 (9)	−0.002 (1)
$\varepsilon_y(2\mathbf{q})$, $\varepsilon_y(4\mathbf{q})$	−0.0364 (9)	0.003 (1)
$\varepsilon_z(2\mathbf{q})$, $\varepsilon_z(4\mathbf{q})$	0.024 (1)	0.013 (2)

The setting for this structure refinement has been changed with respect to the original setting of Bevan *et al.* (1990) in order to be compatible with the modulated structure refinements in the analogous zirconium nitride oxide fluoride system. The a and c axes have been interchanged with respect to the earlier refinement, *i.e.* **a** is the layer stacking direction, while **c** represents the modulation direction. The data collection was performed in parts. Parent reflections and various orders of satellite reflections were collected separately using software that was developed to enable data collection for incommensurately modulated crystals on a Philips PW1100/20 diffractometer (Grigg & Barnea, 1993). Up to fourth-order satellite reflections were collected. None of these fourth-order satellite reflections were observed. No attempt was therefore made to collect satellites of order higher than four.

Lorentz–polarization and absorption corrections were performed using the program package *Xtal*3.2 (Hall *et al.*, 1992). The three standard reflections measured every 120 min showed no significant change in intensity. Averaging the reflection intensities in Laue symmetry *mmm* gave 338 unique reflections ($R_{\rm int}$ = 0.050; 0.12 before absorption correction). Other important parameters for the data collection are given in Table 1.

4. Refinement details

The modulated structure refinements were carried out using the software package *JANA*96 (Petříček & Dušek,

Table 4. *Atomic displacement parameters (Å²)*

	U^{11}	U^{22}	U^{33}
Y	0.0092 (2)	0.0106 (2)	0.0118 (2)
O	0.012 (2)	0.008 (1)	0.011 (1)
F	0.011 (2)	0.014 (2)	0.023 (3)

1996). Scattering factors for neutral atoms were taken from *International Tables for Crystallography* (Wilson, 1992). Refinement using full-matrix least-squares was on *F*. An additional uncorrelated uncertainty of 0.01 was included with the counting statistic estimate in the evaluation of weights (see Table 2). Atoms were refined with anisotropic atomic displacement parameters. The anion positions in the *Q* substructure were occupied with 0.826 O + 0.174 F.

The structure was refined as an incommensurate composite structure with the parameter δ chosen as zero. The starting model for the refinement of the structure (*i.e.* average positions and starting values for displacive modulation wave amplitudes) was taken from the previously published structure of $Zr_9(N,O,F)_{20}$ (Schmid & Withers, 1995). In the first step only the average substructures were refined using both sets of parent reflections. Then the major displacive modulation wave amplitude for each of the atoms, *i.e.* $\varepsilon_{My}(\mathbf{q}_Q)$, $\varepsilon_{Ax}(\mathbf{q}_Q)$ and $\varepsilon_{Ax}(\mathbf{q}_H)$, was added and refined starting with the value as derived from $Zr_9(N,O,F)_{20}$ and using parent and first-order satellite reflections of both substructures. All possible sign combinations for these modulation wave amplitudes were tested in the refinement. The correct combination of signs resulted in significantly lower *R* values than any of the other possibilities. The remaining modulation wave amplitudes were then released for refinement with ± 0.0001 as starting values. False minima were investigated by systematically reversing the sign of various modulation wave amplitudes. In each case the refinement self-corrected, *i.e.* the corresponding amplitudes reversed sign to return to their original values. The refinement converged to a final overall *R* value of 0.025 once an isotropic extinction correction had been incorporated (see Tables 1 and 2). Final refined parameters for the average substructures and displacive modulation wave amplitudes are given in Table 3. Atomic displacement parameters are given in Table 4.†

The lack of observed higher-order satellite reflections (no satellite reflections of order higher than $n = 3$, $n = \min(|m_Q|, |m_H|)$, were observed) suggests that the relative origin of the two substructures, *i.e.* δ, must be an unrefineable parameter (see, for example, Pérez-Mato, 1991). Nevertheless, the structure was also refined as a commensurate composite modulated structure. Note that the possible three-dimensional supercell space-group symmetries of $(Y_{17}F_3O_{14})F_{20}$, where c_Q/c_H apparently equals 20/17 (1.1765...) exactly, can be derived from the superspace-group symmetry given in §2 (see Yamamoto & Nakazawa, 1982; Wiegers *et al.*, 1990) and are given by $A2/b11$ (for $\delta = 2N/68$, N an integer), $Ab2m$ [for $\delta = (2N + 1)/68$] and $Ab11$ (otherwise). For a magnitude of the wavevector of 1.174 the closest rational fraction equals 23/27. This ratio results in different three-dimensional space groups and exemplifies the arbitrariness of assigning three-dimensional space groups in such systems. The refinement statistics for the incommensurate modulated model and commensurate modulated models with different values of δ are identical, suggesting the structure is truly incommensurate.

† A list of structure factors has been deposited with the IUCr (Reference: BR0072). Copies may be obtained through The Managing Editor, International Union of Crystallography, 5 Abbey Square, Chester CH1 2HU, England.

Table 5. *Apparent valences*

Site	AV (this work)	AV (Bevan *et al.*, 1990)
*M*1	2.912	2.617
*M*2	2.950	3.589
*M*3	3.103	2.762
*M*4	3.049	3.185
*M*5	2.926	2.656
*M*6	2.915	3.215
*M*7	2.918	2.982
*M*8	2.993	2.884
*M*9	3.125	3.292
O1	1.852	1.744
O2	1.849	2.028
O3	1.897	1.956
O4	1.929	1.851
O5	1.875	1.813
O6	1.847	1.941
O7	1.850	1.949
O8	1.858	1.841
O9	1.917	1.983
F1	0.912	0.996
F2	0.953	0.974
F3	0.963	0.908
F4	0.901	0.951
F5	0.919	0.933
F6	0.974	0.981
F7	0.935	0.930
F8	0.917	0.896
F9	0.972	0.896
F10	0.941	0.901
F11	0.897	0.865

Note: AV's calculated with 14/17 O + 3/17 F on oxygen sites, *i.e.* $R_{ij}^0 = 1.995$ and expected valence 1.824. Distances up to 4 Å have been taken into account.

5. Results and discussion

5.1. *Structure*

Fig. 3(*a*) shows a projection of the structure down *b*. For ease of comparison with Bevan *et al.* (1990) one 'supercell' along *c* ($c = 17c_Q = 20c_H$) is shown. This origin corresponds to $\delta = 0.25$, resulting in a supercell space-group symmetry of $Ab2m$. It is readily seen that the F

atoms are strongly displaced from the average position along the *a*, *i.e.* layer stacking, direction. The anions in the *Q* substructure are also displaced along the *a* direction, although to a lesser extent. The metals, however, do not move at all along *a* (*cf.* the appropriate AMF's). Displacement of the F atoms along *c* is less easy to see. The projection down *a* in Fig. 3(*b*) shows that the *H* substructure is virtually undistorted along both *b* and *c*, *i.e.* it is an almost perfect 3^6 net in projection along *a*. This 3^6 net, however, is substantially buckled, as can be seen from the large displacement along *a* shown in Fig. 3(*a*). The metal atoms and anions of the *Q* substructure move significantly along *b*, but not along *c*. While the anions in the 4^4 net appear to remain in the centre of the surrounding tetrahedron of metal atoms in projection down *a*, it can be seen in Fig. 3(*a*) that they are significantly displaced from the centre of the tetrahedra along *a*.

5.2. *Atomic modulation functions*

The refined displacive atomic modulation functions (AMF's) for the final model as a function of $t_Q = (\mathbf{q}_Q.\mathbf{T}_Q - \delta)$ modulo an integer for the *Q* substructure and as a function of $t_H = (\mathbf{q}_H.\mathbf{T}_H + 1/\gamma\delta)$ modulo an integer for the *H* substructure are shown in Figs. 4(*a*)–(*c*). Note that Y occupies the *M*1 site and (O,F) the *A*1 site of the *Q* substructure, while the *A*1 site of the *H* substructure is occupied by F. The Y atoms of the *Q* substructure show a large modulation amplitude only along the **b** direction, whereas the anions of the *Q* substructure are significantly modulated along both **a** and **b** directions. The F atoms of the *H* substructure show the strongest modulation along the **a** direction, with an amplitude that is ~60% larger than the amplitude in the corresponding zirconium nitride oxide fluoride. However, there are also significant modulations along **b** and **c**, which is in contrast to the structure of $Zr_9(N,O,F)_{20}$, where only the modulation along **a** is strong. The explanation for this difference can be sought in the different sizes of Zr and Y and N and O, respectively. The cell dimensions of the yttrium phase are significantly larger and so is the yttrium–fluorine bond distance when compared with the zirconium–fluorine bond distance. At the same time, however, the metal–metal separation distance around the fluorine layer in the average structure is smaller in the yttrium phase (~1.3% when compared with $Zr(N,O,F)_x$, x = 2.185). Therefore, the F atoms in the yttrium compound have to move substantially further than in the zirconium compound to satisfy their bonding requirements.

Fig. 5 shows the variation in the coordination sphere of Y as a function of $(\mathbf{q}_Q.\mathbf{T}_Q - \delta)$ modulo an integer. Each Y atom is coordinated by four O/F atoms within the same substructure. The distances between the Y atoms and these anions in the *Q* substructure (the dotted lines) do not show a large variation (< 0.1 Å) between minimum and maximum values. The distances between Y and the F atoms in the H substructure (the solid lines) show a large variation between a minimum distance and infinity owing to the fact that the two substructures literally shift past each other resulting in a continuously changing coordination sphere. This distance variation leads to overall metal coordination ranging from 6 to 8 with clearly quite flexible coordination polyhedra.

5.3. *Apparent valence calculations*

Apparent valences (AV's; Brown & Altermatt, 1985; O'Keeffe, 1989) are often an extremely useful guide to the reliability of refined crystal structures. AV's were

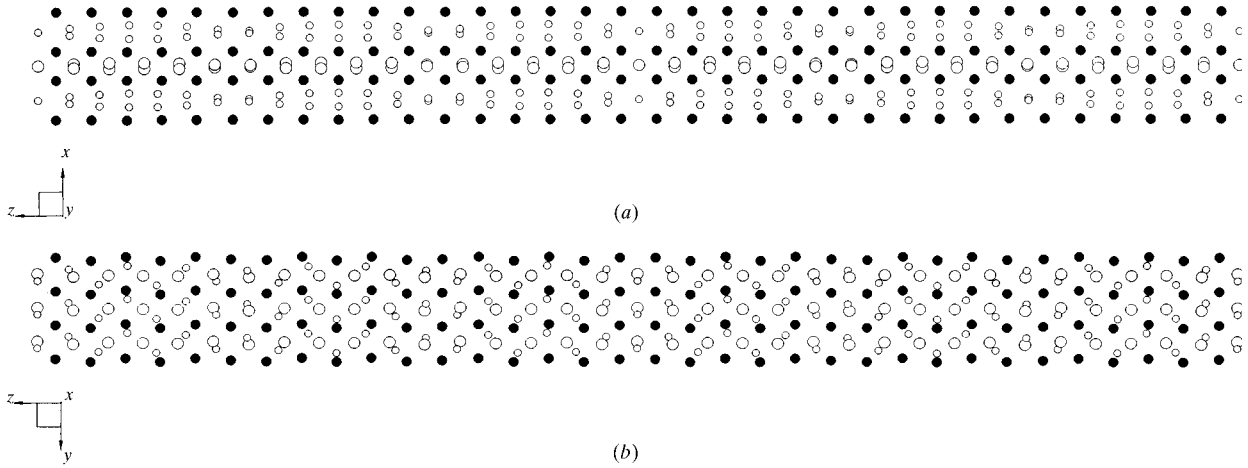

Fig. 3. (*a*) A projection of the structure down *b*. One 'supercell' along *c* ($c = 17c_Q = 20c_H$) is shown. **a** up the page, **c** to the right. *Q* substructure atoms are shown as filled circles (Y) and large open circles (O/F) and *H* substructure atoms as small open circles. (*b*) A projection of part of the structure down *a*. **b** up the page, **c** to the right. *Q* substructure atoms are shown as filled circles (Y) and large open circles (O/F) and *H* substructure atoms as small open circles.

calculated for Y, F and O atoms in the modulated structure using the program *GRAPHT* within the *JANA*96 package (Fig. 6; Petříček & Dušek, 1996). $R^0_{ij}(Y^{3+}-O^{2-})$ = 2.014 Å and $R^0_{ij}(Y^{3+}-F^{-})$ = 1.904 Å (Brese & O'Keeffe, 1991) were used, with the average anion site occupancy in the Q substructure taken into consideration appropriately. The resulting AV's gave no indication of anion ordering within the Q substructure.

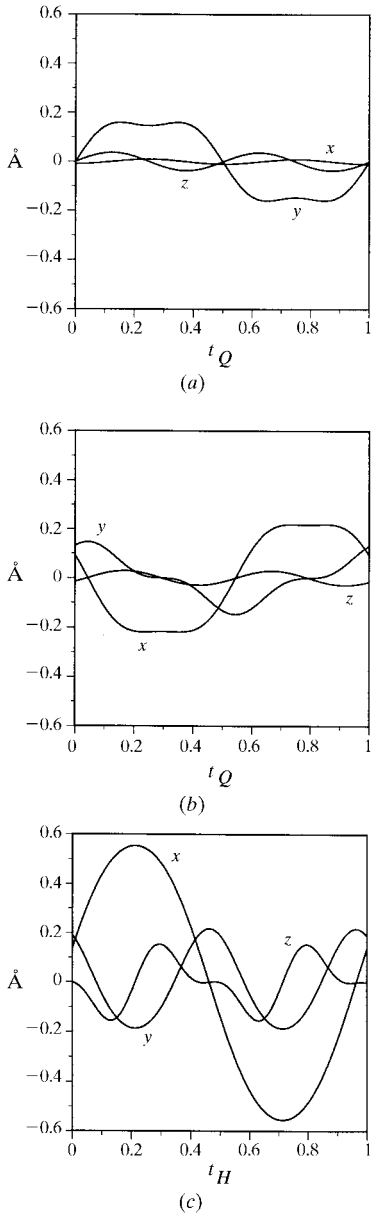

Fig. 4. (*a*) Final refined metal AMF's, *i.e.* U^x_{M1}, U^y_{M1} and U^z_{M1}, plotted in absolute coordinates as a function of $t_Q = (\mathbf{q}_Q.\mathbf{T}_Q - \delta)$ modulo an integer. (*b*) Final refined Q substructure anion AMF's, *i.e.* U^x_{A1}, U^y_{A1} and U^z_{A1}, plotted in absolute coordinates as a function of $t_Q = (\mathbf{q}_Q.\mathbf{T}_Q - \delta)$ modulo an integer. (*c*) Final refined H substructure anion AMF's, *i.e.* U^x_{A1}, U^y_{A1} and U^z_{A1}, plotted in absolute coordinates as a function of $t_H = (\mathbf{q}_H.\mathbf{T}_H + 1/\gamma\delta)$ modulo an integer.

The mean AV for the metal sites is around 3 ± 0.1. For the O atoms one finds approximately 1.87 ± 0.06 and for the fluorine positions in the H substructure one finds about 0.94 ± 0.04. The AV's for the Q substructure anion sites are close to the expected values for a random distribution of anions in the Q substructure, *i.e.* 1.824.

5.4. *Comparison with $Y_{17}O_{14}F_{23}$*

One equally interesting aspect of such structure refinements is the direct comparison of parameters with those of a superstructure refinement. To this end coordinates in a supercell have been calculated from the modulated structure. These coordinates have already been used to draw the structural pictures in Figs. 3(*a*) and 3(*b*). They are also used to calculate AV's. These are given in Table 5 together with those calculated for the

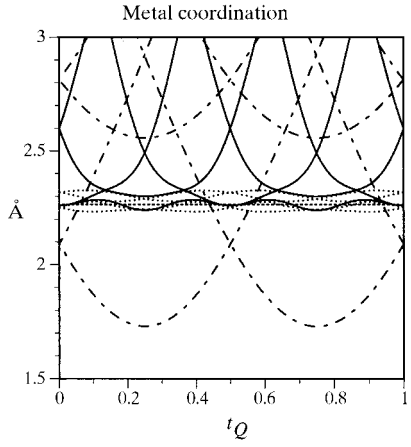

Fig. 5. The variation in the coordination sphere of Y as a function of $t_Q = (\mathbf{q}_Q.\mathbf{T}_Q - \delta)$ modulo an integer. The distances between the Y's and the anions in the Q substructure are shown by dotted lines, whereas the distances between the Y and the F atoms in the H substructure are shown by solid lines. The dot–dashed lines show the distance variation in the unmodulated structure.

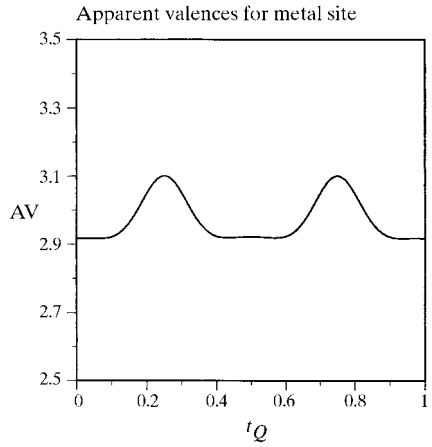

Fig. 6. The variation for the AV of Y as a function of $t_Q = (\mathbf{q}_Q.\mathbf{T}_Q - \delta)$ modulo an integer. It is readily seen that there is only an insignificant variation around the ideal value of 3.

structure of $Y_{17}O_{14}F_{23}$ (Bevan *et al.*, 1990; Schmid & Withers, 1994). It is readily seen that the spread of values that existed in the superstructure refinement has virtually disappeared. Comparing the actual coordinates shows that only very few atoms have moved more than a few picometers. This again highlights the advantage of a modulated structure approach which constrains the atoms to move in a sensible fashion, taking into account the information contained in reciprocal space.

On the basis of their bond-valence sums Bevan *et al.* (1990) discussed the possibility of anion ordering in the *Q* substructure with subsequent lowering of space-group symmetry. Given the narrow spread of the AV's for all atom positions in this refinement, such anion ordering and lowering of space-group symmetry does not seem to be required for an understanding of the structure.

The overall *R* value for the modulated structure refinement is substantially lower than for the superstructure refinement (0.025 compared with 0.101), while employing a vastly reduced number of positional parameters (17 compared with 80). It needs to be pointed out, however, that Bevan *et al.* (1990) used approximately twice as many reflections for their refinement. This suggests that many of these were not really significant, as from a modulated structure perspective there should not be a large variation in the number of observed reflections on going from one composition to another.

6. Conclusions

A composite modulated structure approach has been used to re-refine and describe the structure of $(YO_{1-\Delta}F_{\Delta})F_{1+\Delta}$, $\Delta = 0.174$. Starting values for the displacive modulation wave amplitudes used in the refinement were derived from a previously reported structure refinement of a chemically different but 'isostructural' phase. Refinement in terms of modulation waves shows the extraordinary similarity of the structures in general terms, but also reveals subtle differences not previously noted. While the published superstructure refinement represents a good approximation, the modulated structure approach allows a better control of the refinement and a more elegant description of the structure and indeed the whole solid solution.

The author wishes to express his gratitude to Professor D. J. M. Bevan for the supply of single crystals used for data collection and acknowledges many fruitful discussions with Dr R. L. Withers.

References

Bevan, D. J. M. & Mann, A. W. (1975). *Acta Cryst.* B**31**, 1406–1411.

Bevan, D. J. M., Mohyla, J., Hoskins, B. F. & Steen, R. J. (1990). *Eur. J. Solid State Inorg. Chem.* **27**, 451–465.

Brese, N. E. & O'Keeffe, M. (1991). *Acta Cryst.* B**47**, 192–197.

Brown, I. D. & Altermatt, D. (1985). *Acta Cryst.* B**41**, 244–247.

Grigg, M. W. & Barnea, Z. (1993). *Software Amendments for Philips PW*1100/20. School of Physics, University of Melbourne, Melbourne, Australia.

Guinier, A. (1984). *Acta Cryst.* A**40**, 399–404.

Hall, S. R., Flack, H. D. & Stewart J. M. (1992). Editors. *Xtal*3.2 *Reference Manual*. Universities of Western Australia, Australia, Geneva, Switzerland, and Maryland, USA.

Hyde, B. G., Bagshaw, A. N., Andersson, S. & O'Keeffe, M. (1974). *Ann. Rev. Mater. Sci.* **4**, 43–92.

Janssen, T., Janner, A., Looijenga-Vos, A. & de Wolff, P. M. (1992). *International Tables for Crystallography*, Vol. C, edited by A. J. Wilson, pp. 797–835. Dordrecht: Kluwer Academic Publishers.

Jung, W. & Juza, R. (1973). *Z. Anorg. Allg. Chem.* **399**, 129–147.

Makovicky, E. & Hyde, B. G. (1981). *Struct. Bonding*, **46**, 101–170.

Makovicky, E. & Hyde, B. G. (1992). *Non-Commensurate Layered Structures*, edited by A. Meerschaut, pp. 1–100. Switzerland: Trans. Tech. Publications.

Mann, A. W. & Bevan, D. J. M. (1972). *J. Solid State Chem.* **5**, 410–418.

O'Keeffe, M. (1989). *Struct. Bonding*, **71**, 161–190.

Pérez-Mato, J. M. (1991). *Methods of Structural Analysis of Modulated Structures and Quasicrystals*, edited by J. M. Pérez-Mato, F. J. Zúñiga & G. Madariaga, pp. 117–128. Singapore: World Scientific.

Pérez-Mato, J. M., Madariaga, G., Zúñiga, F. J. & Garcia Arribas, A. (1987). *Acta Cryst.* A**43**, 216–226.

Petříček, V. & Dušek, M. (1996). *JANA*96. *Programs for Modulated and Composite Crystals*. Institute of Physics, Praha, Czech Republic.

Schlichenmaier, R., Schweda, E., Strähle, J. & Vogt, T. (1993). *Z. Anorg. Allg. Chem.* **619**, 367–373.

Schmid, S., Fütterer, K. & Thompson, J. G. (1996). *Acta Cryst.* B**52**, 223–231.

Schmid, S., Thompson, J. G., Withers, R. L., Petříček, V., Ishizawa, N. & Kishimoto, S. (1997). *Acta Cryst.* B**53**, 851–860.

Schmid, S. & Withers, R. L. (1994). *J. Solid State Chem.* **109**, 391–400.

Schmid, S. & Withers, R. L. (1995). *Acta Cryst.* B**51**, 746–753.

Schmid, S. & Withers, R. L. (1996). *Aust. J. Chem.* **49**, 827–833.

Smaalen, S. van (1991). *Phys. Rev. B*, **43**, 11330–11341.

Smaalen, S. van (1995). *Cryst. Rev.* **4**, 79–202.

Wiegers, G. A. (1996). *Prog. Solid State Chem.* **24**, 1–139.

Wiegers, G. A., Meetsma, A., Haange, R. J., van Smaalen, S., de Boer, J. L., Meerschaut, A., Rabu, P. & Rouxel, J. (1990). *Acta Cryst.* B**46**, 324–332.

Wilson, A. J. (1992). Editor. *International Tables for Crystallography*, Vol. C. Dordrecht: Kluwer Academic Publishers.

Withers, R. L., Schmid, S. & Thompson, J. G. (1993). *Acta Cryst.* B**49**, 941–951.

Wolff, P. M. de, Janssen, T. & Janner, A. (1981). *Acta Cryst.* A**37**, 625–636.

Yamamoto, A. (1996). *Acta Cryst.* A**52**, 509–560.

Yamamoto, A. & Nakazawa, H. (1982). *Acta Cryst.* A**38**, 79–86.